Thin-Walled Structures 91 (2015) 29–37

Contents lists available at ScienceDirect

Thin-Walled Structures

journal homepage: www.elsevier.com/locate/tws

Buckling estimates for oil storage tanks: Effect of simplified modeling of the roof and wind girder

Carlos A. Burgos [a], Jean C. Batista-Abreu [b], Horacio D. Calabró [a], Rossana C. Jaca [a], Luis A. Godoy [c,*]

[a] Facultad de Ingeniería, Universidad Nacional del Comahue, Neuquén, Argentina
[b] Johns Hopkins University, Baltimore, Maryland, USA
[c] Institute for Advanced Studies in Engineering and Technology, CONICET-FCEFyN, Universidad Nacional de Córdoba, Argentina

ARTICLE INFO

Article history:
Received 28 November 2014
Received in revised form
6 February 2015
Accepted 6 February 2015

Keywords:
Finite element analysis
Pressure
Shells
Tanks
Thermal loads
Wind pressures

ABSTRACT

Oil storage tanks are short cylindrical shells fabricated with an external fixed roof or floating roof on the inside. Some features of the structure tend to be simplified in practice and research in order to perform stability and strength analyses using a much simpler model. This paper considers the structural consequences of such simplifications, including the substitution of a supporting structure of the roof or a wind girder by an equivalent thickness or by a fictitious boundary condition. Three load cases are investigated: thermal loads due to an adjacent fire, uniform external pressure, and wind pressure. Results of finite element analyses to evaluate bifurcation loads and modes are reported as estimates of buckling. Equivalent thickness models are derived by establishing equivalences in moment of inertia or sectional modulus of the components that are not represented in detail. The differences in buckling loads associated with equivalent thickness models depends on the load case considered, but range between 7–15% for a case studied with a fixed roof, with smaller differences (3%) for opened top tanks with wind girders. Substitution of a wind girder by a boundary condition, on the other hand, yields large errors under thermal loads exceeding 80% of buckling loads.

1. Introduction

Liquid-storage tanks have relatively simple geometries, basically a vertical cylindrical shell with a roof, but they often present some additional complexities in practice. Depending on the diameter of the cylinder, tanks may have a fixed roof or a floating roof, or may be opened at the top. There are also tanks having both floating and fixed roofs.

Tanks with a fixed roof are frequently fabricated with a conical or flat roof, which are not self-supported but require of an additional supporting structure: a three dimensional grid formed by rafters, rings, and columns, as shown in Fig. 1. In the example of Fig. 1 there are two intermediate rings that delimitate three annular regions on the roof; 16 rafters run through the three regions, 16 additional rafters span the second and third annular sectors, and 32 rafters are added in the third sector, so that altogether there are 64 rafters in the third sector. A typical cross-section of a rafter is shown in Fig. 1c, taken from a real tank located in USA.

Because of the complexity added by the grid of rafters and rings, researchers and designers attempt to simplify the structural analysis by eliminating the three dimensional grid and substituting it by a modification in the thickness of the roof. Such "equivalent" roof is a self-supported shell with a modified thickness, but also the weight needs to be adjusted in order to avoid having an excessively heavy roof which would buckle under self-weight. This approach may be found in many research papers, such as Refs. [1–5]. Even simpler models have been considered in the literature, in which the roof is completely eliminated and its influence is represented by simply supported boundary conditions at the top of the cylindrical shell [6]. Such simplifications are not motivated by computer time constraints, but are frequently made to simplify modeling and data entry.

Open top tanks, on the other hand, are usually designed with a wind girder at the top to provide stability to the cylindrical shell and thus avoid snap-through buckling. Design provisions in the United States [7] and Europe [8] provide guidance regarding the cross-sectional shapes of wind girders. Such girders have been taken into account in some research papers [9,10,11], whereas they have not been included in the analysis by other researchers [12]. Simplifications to eliminate a wind girder from a model include substitution by boundary conditions to restraint radial

* Corresponding author.
E-mail address: lgodoy@efn.uncor.edu (L.A. Godoy).

http://dx.doi.org/10.1016/j.tws.2015.02.006
0263-8231/

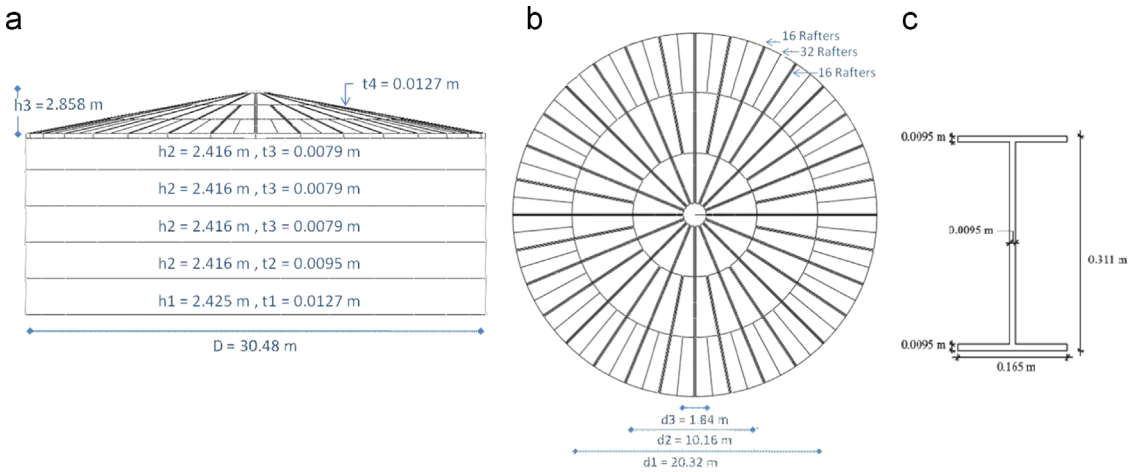

Fig. 1. Geometry of the tank and supporting structure, (a) front view, (b) plane view, and (c) cross-section of rafters.

displacements (such as in Ref. [12]) or substitution by a modified shell thickness in the region where the wind girder should be present.

Because tanks are formed by very thin-walled shells, buckling becomes a major design constraint, and collapses due to environmental actions and accidents have been reported in many occasions in the literature [13–15]. A state of the art on the buckling of shells may be found in the work of the European Convention for Constructional Steelwork (ECCS) [16]; however, the ECCS book employs some of the simplifications mentioned above without further discussion. At present, the ECCS committee is seeking response to such uncertainties and has called for research in this area; this paper is part of such inquiry addressing those topics identified as voids in current knowledge.

Questions arise as to what are the consequences of such simplifications on the buckling behavior of the structure. Are those effects independent of the loading condition, or do they have different effects depending on the nature of the load (i.e., thermal, lateral pressure). This paper addresses these problems in order to elucidate how such simplifications affect buckling of the shell, and specifically considers thermal loads, uniform pressures, and wind pressures as separate loading cases. Case studies are discussed for two tank configurations, namely fixed roof and open top configurations.

2. Tanks with conical roof

2.1. Case study

A specific fixed roof geometry is considered in this section in order to identify the structural consequences of the assumed simplifications. The shell is shown in Fig. 1, with step-wise variable thickness and a conical roof; the overall geometry is given by a diameter $D=30.38$ m, cylinder height $H=12.19$ m, and 2.86 m maximum elevation of the roof with respect to the cylinder. Details of the structural grid supporting the roof are shown in Fig. 1b. The shell thickness as well as the roof structure have been designed according to API 650 regulations [7]. Two equally-spaced intermediate rings were placed between the roof center and its junction with the cylinder. In the outer section there are 64 rafters; 32 rafters in the middle sector, and 16 rafters in the inner sector. The cross-section of the rafters is shown in Fig. 1c. ASTM A36 steel is assumed for all components of the tank, with density $\gamma=7850$ Kg/m^3, elastic modulus $E=206$ GPa, and Poisson's ratio 0.3.

The cylinder was assumed to be fixed at the base. A finite element discretization of the structure was made by means of the general

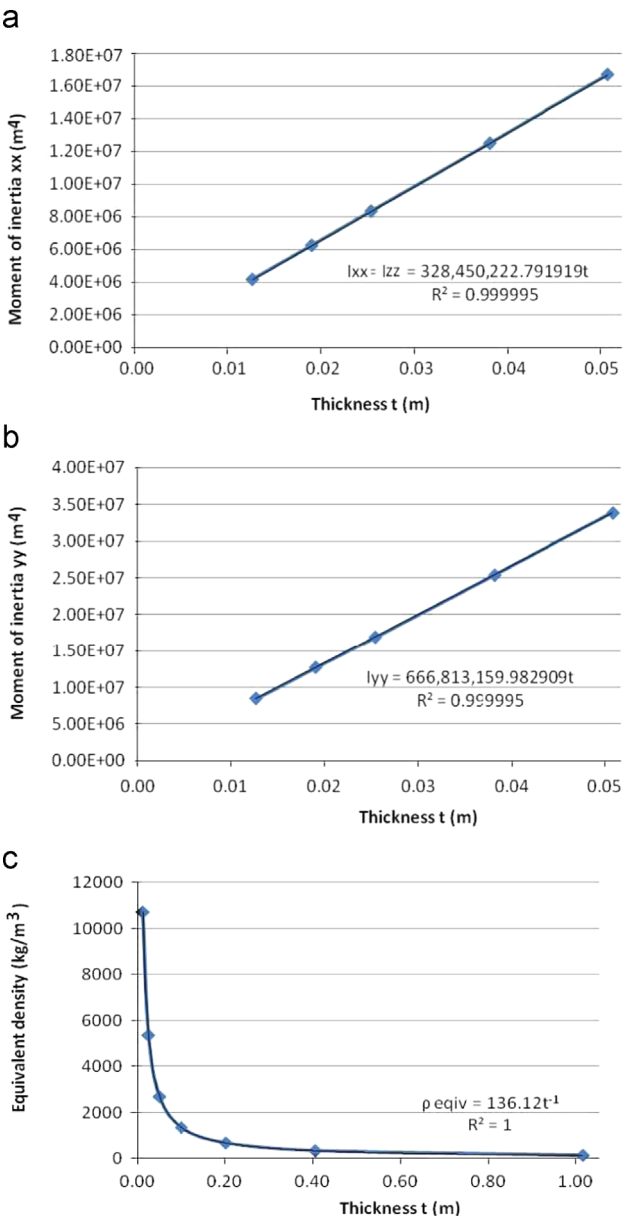

Fig. 2. Self-supported model, (a) inertia $Ixx=Izz$, (b) inertia Iyy, and (c) equivalent density.

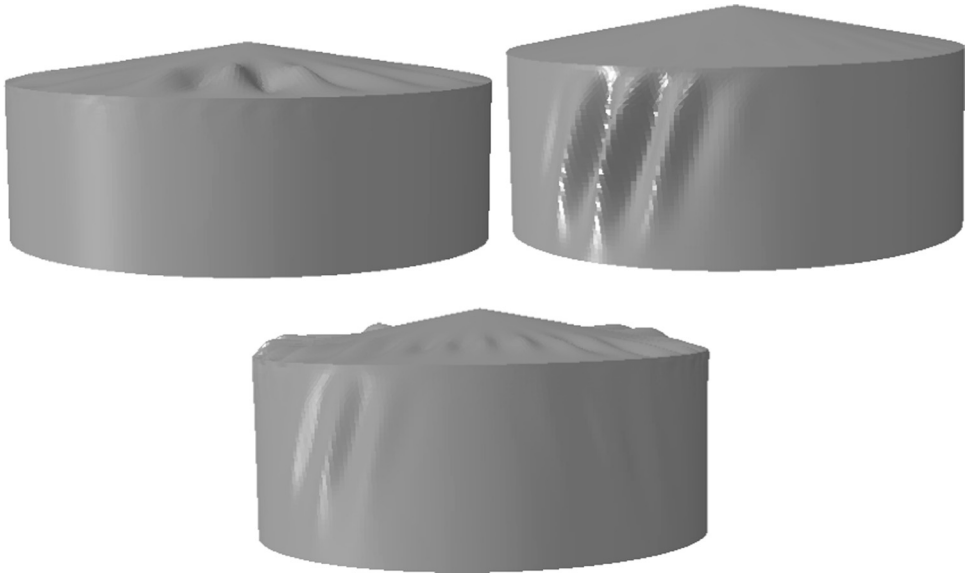

Fig. 3. Critical modes for the tank with roof and supporting structure under thermal load, (a) first roof mode, T^C=94 °C, (b) first cylinder mode, T^C=205 °C, and (c) first combines roof and cylinder mode, T^C=208 °C.

Fig. 4. Buckling mode for tank with equivalent roof thickness, under thermal load.

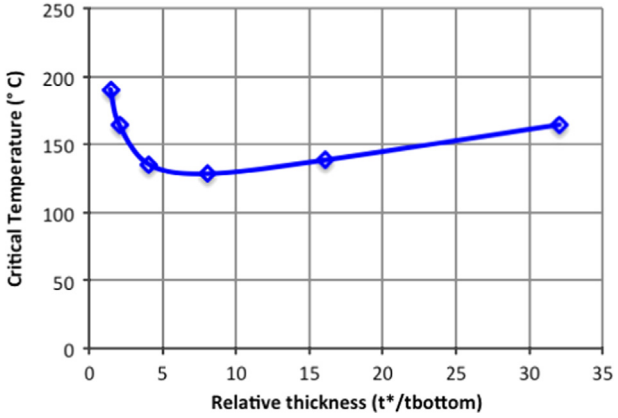

Fig. 5. Critical temperature versus equivalent roof thickness.

purpose program ABAQUS [17]. Eight-node shell elements with reduced integration (identified as S8R5 in ABAQUS) were used for the cylinder, whereas triangular elements were employed on the roof (STRI65). Rafters were represented by beam elements, and columns were not explicitly included in the discretization but vertical restraints were applied at the points where they support the structural grid. Results obtained with this model will be identified as exact models.

The moments of inertia of the exact roof model were evaluated using ABAQUS as follows: there is a facility in ABAQUS to evaluate the inertia of the complete or part of a structure, in which case the density of the material needs to be provided. In this case a unit value of density was employed because this was one of the variables to be adjusted as part of the equivalence. The moments of inertia were computed with respect to the center of mass of the roof. An orthogonal system of coordinates was used for the evaluation of inertias, in which axis *YY* is the vertical direction (the axis of symmetry of the conical roof); whereas axis *XX* and *ZZ* are symmetry axis, so that the moments of inertia with respect to *XX* and *ZZ* are the same value.

Thus, the values of inertia for the specific roof configuration considered were

$$I_{xx} = I_{zz} = 5,846,414 \text{ m}^4$$
$$I_{yy} = 11,869,274 \text{ m}^4 \quad (1)$$

These are the target values which will be used to make equivalence between exact and simplified models.

2.2. Simplifications investigated

A structure with similar dimensions to those considered in the previous section was investigated by assuming a self-supported conical roof (without columns as supporting structure) in which the roof thickness is modified in order to satisfy an equivalence condition in terms of total roof inertia. There is no unique way to establish equivalence relations, and only one is explored in this paper using the equivalence between inertia values.

The same procedure described in the previous section to evaluate the inertia of the exact model was next used for the roof with a uniform thickness. To obtain a parametric representation of the inertia as a function of the shell thickness, reference was made to the thickness of the cylinder in the bottom course indicated in Fig. 1a. For different values of roof thickness, the moment of inertia of the roof was evaluated and results are shown in Fig. 2a and b as a function of roof thickness.

Using regression analysis, the moment of inertia can be written in terms of the thickness at the base of the tank (t_{bottom}) as

$$I_{xx} = I_{zz} = 328,450,223 \ t_{\text{bottom}}$$
$$I_{yy} = 666,813,160 \ t_{\text{bottom}} \quad (2)$$

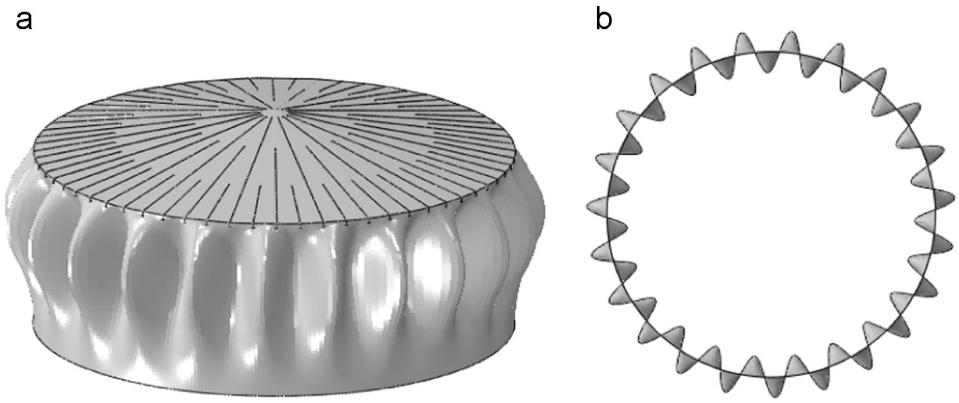

Fig. 6. First critical mode for case studied under uniform pressure (p^C=2.53 kN/m^2), for the exact roof model. (a) Side view and (b) top view.

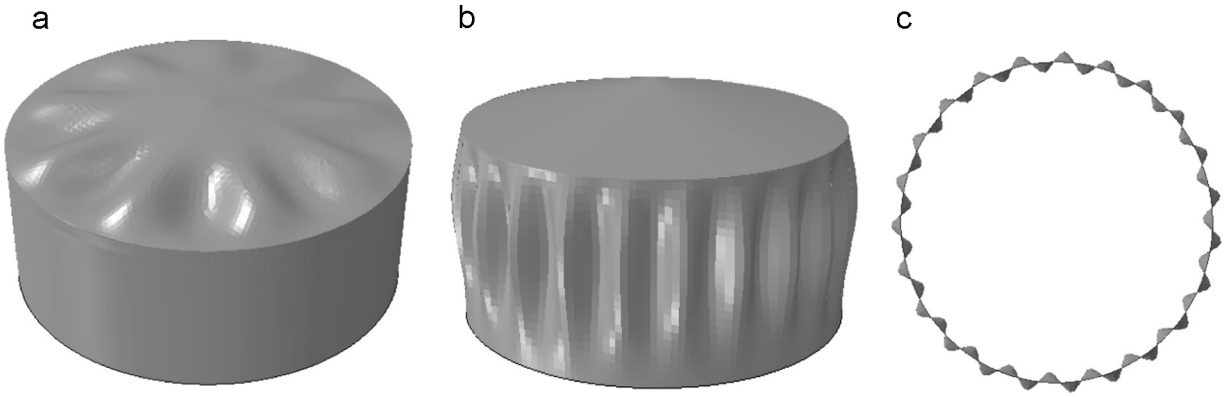

Fig. 7. Tank under uniform pressure, first critical mode for simplified self-supported roof, (a) 1.4 t (p^C=0.81 kN/m^2), (b) 24 t (p^C=2.55 kN/m^2), and (c) 24 t (23 circumferential waves).

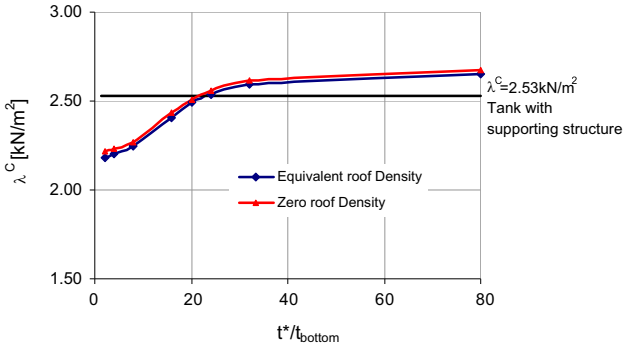

Fig. 8. Critical uniform pressure versus equivalent roof thickness.

The density of the material needs to be adjusted in order to keep the same roof weight. The density in terms of the thickness (Fig. 2c) is

$$\rho_{equiv} = \frac{136.12}{t_{bottom}} \tag{3}$$

The results of inertia for different values of t given in Fig. 2 indicate that the same moment of inertia as in the exact roof model are obtained for an equivalent thickness t^* of 17.8 mm, or

$$t^* = 1.4\ t_{bottom} \tag{4}$$

Alternatively, this may be written in terms of the course thickness at the top of the cylinder as t^*=2.25 t_{top}.

Of course, an equivalence established between moments of inertia does not guarantee that buckling loads will also satisfy equivalence; thus, this needs to be investigated by means of computational modeling of the exact and simplified structure under various loading conditions. This is the subject of the following sections.

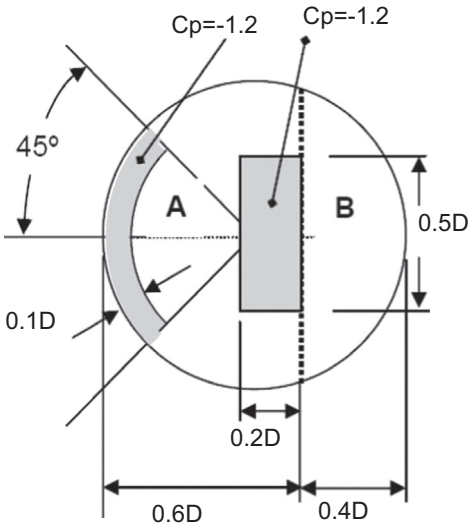

Fig. 9. Assumed wind pressure distribution on the roof [22].

2.3. Buckling under thermal loads

Thermal loads arising as a consequence of an adjacent fire have been investigated by Liu and coworkers [2,18,19]. These authors performed a detailed heat transfer study from the source of fire to the shell, and proposed using a $\cos^2\theta$ variation of temperature in the circumferential direction of the cylinder, where θ is the angular coordinate measured from the meridian of incidence of fire. Fire is assumed to increase temperature on a sector of the shell most directly exposed to the heat source.

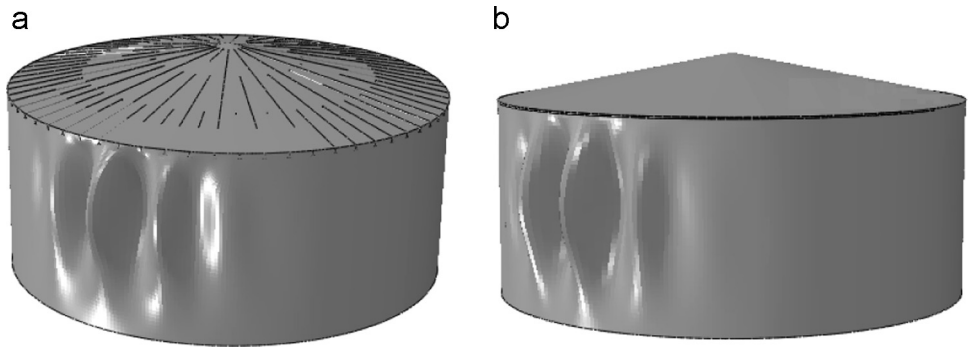

Fig. 10. Tank under wind, first critical mode for the tank, (a) with supporting structure (p^C=3.36 kPa) and (b) self-supported roof t^*=32 t_{bottom}, roof weight neglected (p^C=3.33 kN/m^2).

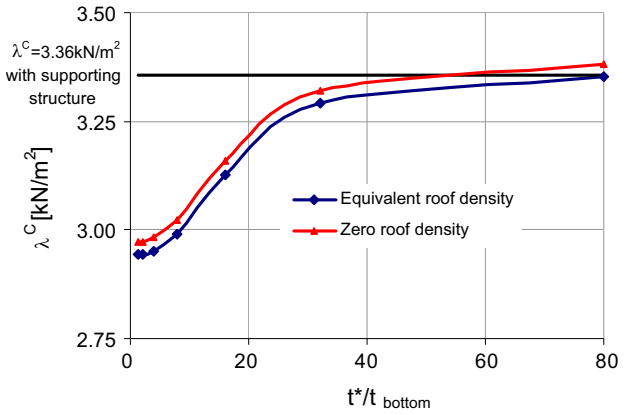

Fig. 11. Critical wind pressures for self-supported model, versus equivalent thickness.

In the research presented in this paper, a sector covering half of the perimeter of the cylinder is assumed to be affected. The temperature distribution is written in the form

$$\begin{cases} T(\theta) = \lambda T_0 \cos^2\theta, & \text{for} \quad -\frac{\pi}{2} \le \theta \le \frac{\pi}{2} \\ T(\theta) = 0, & \text{for} \quad \frac{\pi}{2} \le \theta \le \frac{3\pi}{2} \end{cases} \tag{5}$$

where λ is a scalar multiplier used to increase the reference temperature T_0. The influence of the vertical distribution has been studied by Liu [2] and is here assumed to be uniform in elevation. The influence of the zone affected by heat on the buckling of the shell has been studied in Ref. [20].

Because relative changes for exact and simplified models are investigated in this work, a bifurcation analysis (designated as LBA in Ref. [16]) is computed in each case, in order to have an estimate of buckling load. This yields an eigen-value problem [21]

$$\left(K_0 + \lambda^C K_G\right)\varphi^C = 0 \tag{6}$$

where K_0 is the linear stiffness matrix of the shell, K_G is the load-geometry matrix which includes the nonlinear kinematic relations, the eigenvalue λ^C represents the critical load or temperature at bifurcation, and the eigenvector φ^C is the shell configuration at bifurcation, i.e. the critical mode. Depending on the assumed load condition, the eigenvalue multiplies a temperature or a pressure.

For the tank having an exact roof model, the first mode occurs at a critical temperature $T^C=\lambda^C T_0$ equal to T^C=94 °C and the bifurcation mode is seen to mainly have displacements on the roof (see Fig. 3a). The cylinder shows deflections in another mode for a critical temperature T^C=205 °C (Fig. 3b), whereas deflections on the roof and cylinder are obtained in a mode at T^C=208 °C. Interest in this work focuses on cylinder modes, which may have severe structural consequences by blocking the floating roof on top of the fluid. Thus attention focuses on the mode with T^C=205 °C.

Models with equivalent thickness t^* have been investigated for the same load distribution. For t^*=1.4 t_{bottom}, a critical temperature T^C=191 °C is obtained, with displacements in the cylinder and also in the roof. The bifurcation buckling mode is shown in Fig. 4, and is similar to that obtained for the exact model of the roof. Differences between the simplified (equivalent thickness) and exact roof models are of approximately 7% for this case-study.

To illustrate the influence of t^* on the critical temperature, results for increasing values of t^* normalized with respect to t_{bottom} are presented in Fig. 5. For $1.4 < t^*/t_{bottom} < 8$ there is a decrease in T^C, reaching a low value at T^C=129 °C, with a 37% difference with respect to the exact model. If the value of t^* is further increased to even larger values, the results increase and approach the "exact" value at t^*/t_{bottom}=27. Such large equivalent thickness is unrealistic, but it shows that there are large roof thicknesses for which the same buckling load would be recovered as in the exact roof model. Notice that there are two equivalent thickness values for which the "exact" critical temperature is reached: one is associated with membrane stiffness for small thickness, whereas for large thickness values equivalence is reached by bending stiffness in a thick shell.

2.4. Buckling under uniform pressure

To better understand how the load case considered affects the buckling of a tank with an equivalent roof thickness, the case of uniform external pressure (internal vacuum) has been investigated. The critical pressure is here designated as $p^C=\lambda^C p_0$, where p_0 is a reference unit pressure.

For the exact roof model, a LBA leads to a lowest eigenvalue p^C=2.53 kPa, with an associated eigen-mode shown in Fig. 6. This is symmetric pattern around the circumference, and is characterized by 23 waves, shown in Fig. 6b.

The equivalent thickness model has next been computed for t^*=1.4 t_{bottom}: it displays a roof mode (shown in Fig. 7a), with a low value of p^C=0.81 kPa. The first mode for which a cylinder mode occurs is t^*=2.0 t_{bottom}, in which case p^C=2.18 kPa (14% difference with respect to the "exact" case).

Parametric studies have been performed by increasing t^*. The results of Fig. 8 indicate that the critical pressure increases and reaches the "exact" values at t^*=24 t_{bottom}. The eigen-mode for t^*=24 t_{bottom} is shown in Fig. 7b and c, having 23 full waves in the circumferential direction.

Results are also compared in Fig. 8 between models with an equivalent density (as in Fig. 3c) versus models in which self-weight of the roof is neglected. The eigenvalues p^C are only marginally affected by the roof weight, and either assumption provides similar results.

2.5. Buckling under wind pressures

The simplifications regarding the roof are next studied under wind pressures. There are a number of proposals in the literature to represent a static pressure due to wind in vertical cylindrical structures; in this paper the assumed pressures follow the Australian regulations [22]: the external pressure coefficient C_p around the circumference of a cylinder is given by

$$Cp(\theta) = k_c Cp_1(\theta)$$
$$Cp_1(\theta) = -0.5 + 0.4\cos\theta + 0.8\cos 2\theta + 0.3\cos 3\theta - 0.1\cos 4\theta - 0.05\cos 5\theta \quad (7)$$

where θ is the central angle measured from the windward meridian. Factor k_c takes the form

$$k_c = 1.0 - 0.55(Cp_1 + 0.15)\log(H/D) \quad \text{for } Cp_1 < -0.15 \quad (8)$$

A uniform pressure distribution in elevation is adopted according to this code. The pressure distribution on the conical roof is shown in Fig. 9, with $C_p = -0.8$ in region A and $C_p = -0.5$ in Region B. In all cases, negative coefficients indicate suction and positive coefficients indicate pressure.

Analysis of the tank with a supported conical roof has been performed using the same finite element mesh previously employed. Under wind pressures, the shell reaches a bifurcation load computed via LBA at $p^C = 3.36$ kPa, which is higher than what is obtained under uniform pressure. The eigen-mode is shown in Fig. 10, mainly affecting the cylindrical body of the structure, with large deflections in the windward region.

Results for a self-supported roof with an equivalent thickness has been computed for $t^* = 1.4\ t_{bottom}$, leading to $p^C = 2.94$ kPa, a value 12% lower than the "exact" value considering the exact roof model.

For increasing values of equivalent thickness, the results have been plotted in Fig. 11: as the thickness increases, the gap between the "exact" and approximate solutions becomes smaller, and coincidence is reached for $t^* = 40\ t_{bottom}$. Two conditions have been considered: with a modified density of the equivalent roof and neglecting the roof weight. Both conditions yield approximately the same results.

The mode shapes obtained with the simplified models are similar to that computed in the supported roof structure.

3. Tanks opened at the top

3.1. Case studied

The specific tank considered in this section is shown in Fig. 12, with $D = 37.9$ m and $H = 9.47$ m, and step-wise variable thickness. There is a wind girder at the top in order to restraint displacements in the upper part of the tank. The dimensions of the wind girder are shown in Fig. 13a, and were designed according to API 650 [7]. This is one of the typical stiffening ring sections for tank shells illustrated in API 650 (see Detail e in Figure 5.24 of API 650 [7]). The minimum thickness of the shell is $t_{top} = 9.5$ mm, with a maximum $t_{bottom} = 12.7$ mm. The same empirical expression is given in API 650 and BS 2654 [8] to calculate the minimum sectional modulus W of the wind girder in the form

$$W = \frac{D^2 H}{17} \quad (9)$$

for wind velocities of 190 km/h. In the present case, a wind velocity of 165.6 km/h has been assumed for the northern part of Patagonia in Argentina, so that the value of W needs to be adjusted by the factor $(165.6/190)^2$. The assumed material properties are the same as in the tank with a fixed roof.

For the thickness of the top course (which is 9.5 mm in the present case), API 650 indicates that a stiffener should be designed as indicated by detail e of Figure 5.24 in API 650 [7]. This yields a value of $W = 607.85$. Table 5.20 in the same document API 650 provides possible dimensions to be adopted by the designer. In this case, for $b = 40$ mm, the API table gives a modulus $W_{adop} = 723$ cm^3, which has been adopted in the present case.

3.2. Simplifications investigated

Two simplifications have been considered in this case-study: one of them substitutes the wind girder by an "equivalent" thickness at the top of the shell in the region where the ring is located. The equivalence is established by equating the moment of inertia with respect to a vertical axis of the tank sector with the wind girder shown in Fig. 13b, with the inertia of the same sector with an equivalent thickness ($h = 0.31$ m). For this case studied, the equivalent thickness is 4.75 t_{top}.

A second simplified model has been investigated by eliminating the wind girder and adding boundary conditions at the top to prevent radial displacements.

Bifurcation loads and modes were computed using the same software and finite elements as in the tank with a fixed roof. Convergence studies were performed to identify a suitable finite element mesh, resulting in elements of 0.2 m height for the cylinder, which were reduced to 0.1 m at the top course.

3.3. Buckling under thermal load

The effects of structural simplifications on open top tanks under thermal loads were investigated under the same temperature distribution around the circumference and in elevation as discussed in Section 2.3.

For the model with a wind girder, the lowest critical temperature was $T^C = 267$ °C. The eigen-mode, given in Fig. 14, has displacements at the bottom of the shell in the region of incidence of fire.

Results for the simplified shell with an equivalent thickness were the same, i.e. $T^C = 267$ °C, with the shape at bifurcation shown in Fig. 15a. The mode is clearly the same as in the tank with the wind girder, so that this represents an excellent approximation.

The model in which the girder is substituted by boundary conditions, on the other hand, provided a low value of $T^C = 74$ °C, with a bifurcation mode (Fig. 15b) showing a different patterns of

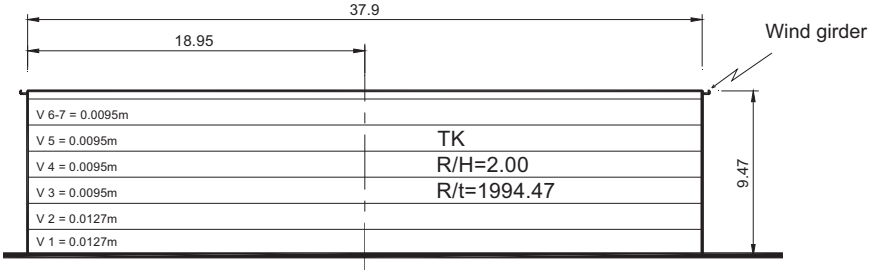

Fig. 12. Geometry of opened tank investigated.

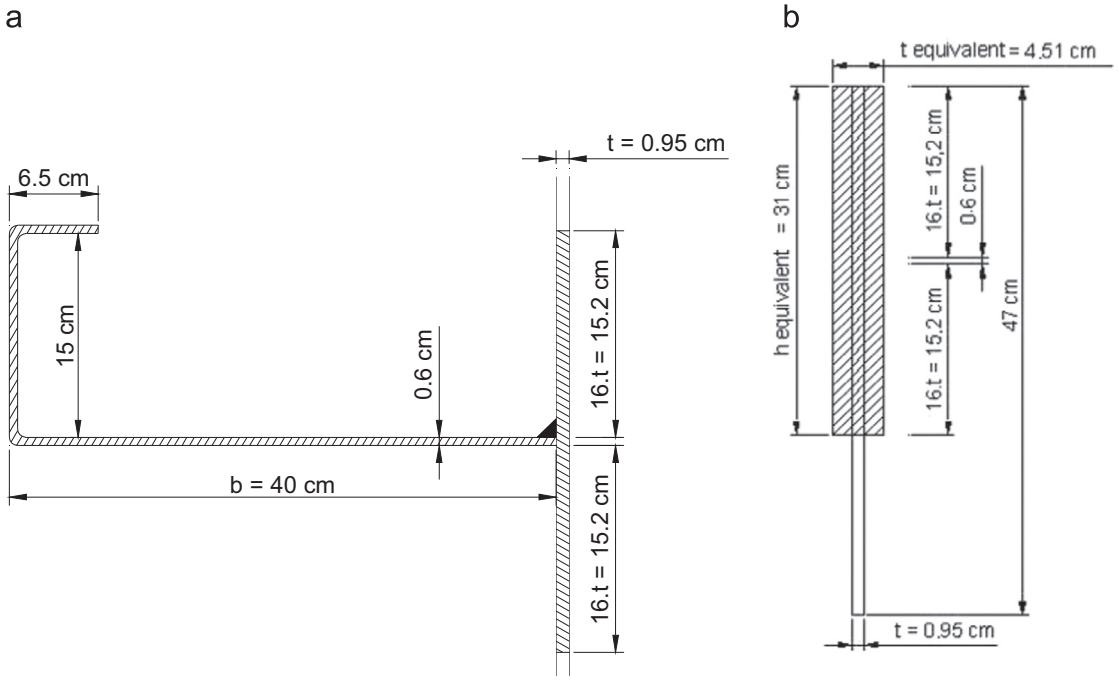

Fig. 13. Wind girder (a) details of wind girder and (b) simplified model with equivalent thickness.

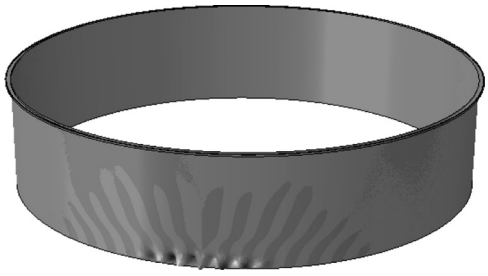

Fig. 14. First critical mode for tank with wind girder (T^C=266.9 °C).

deflections (given by symmetric bulges on a large circumferential zone and ranging from top to bottom in elevation) than the "exact" model. Problems under thermal loading are sensitive to the constraints enforced on displacements: more stringent displacement constraints, as in the fictitious boundary conditions model, do not allow realistic displacements under temperature and yield very low buckling loads. Not just the critical temperature but also the bifurcation mode are seen to significantly differ from what is obtained in an "exact" wind girder model.

3.4. Buckling under uniform pressure

The tank with a wind girder, under lateral uniform pressure, has a critical pressure at p^C=3.14 kPa, with the mode shape having 28 full waves around the circumference (Fig. 16).

The simplified model with an equivalent thickness yields p^C=3.25 kPa, which is 3.5% higher than the "exact" result. The associated eigenmode is shown in Fig. 17b and c, and is almost coincident with the exact mode, again having 28 full circumferential waves.

For the model with boundary conditions at the top, a critical p^C=3.06 kPa is computed, a value 2.5% lower than the tank with a wind girder. The bifurcation mode again has 28 full waves around the circumference (Fig. 17a).

Because of the small differences with the exact value, parametric studies for different values of W in the equivalent thickness model have not been performed.

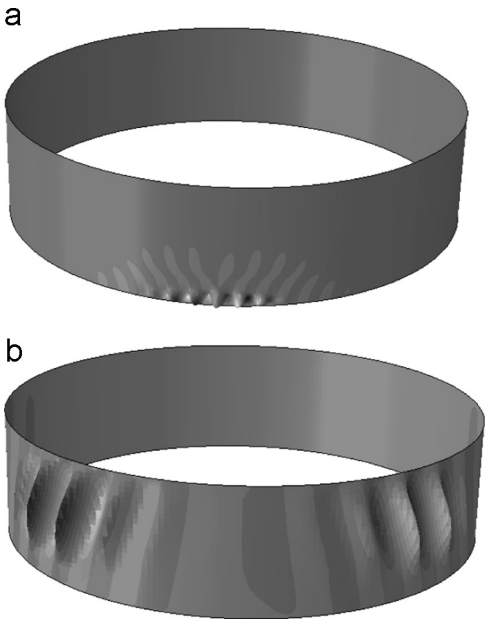

Fig. 15. First critical mode, (a) equivalent thickness model (T^C=266.9 °C) and (b) simplified model with boundary conditions at the top (T^C=74 °C).

3.5. Buckling under wind pressure

To investigate buckling under wind, the same standard [22] has been used as in the fixed roof case. The same pressure distributions are employed in the circumference and in elevation, but a suction coefficient 0.18 is added to account for the tank being opened at the top.

For the tank with wind girder, the critical pressure reaches p^C=3.38 kPa, which is slightly higher than under uniform pressure. The shape of the structure at bifurcation buckling is shown in Fig. 18a, affecting just the zone at windward.

The tank with equivalent thickness in this case leads to p^C=3.47 kPa (a value 2.7% higher); whereas the model with

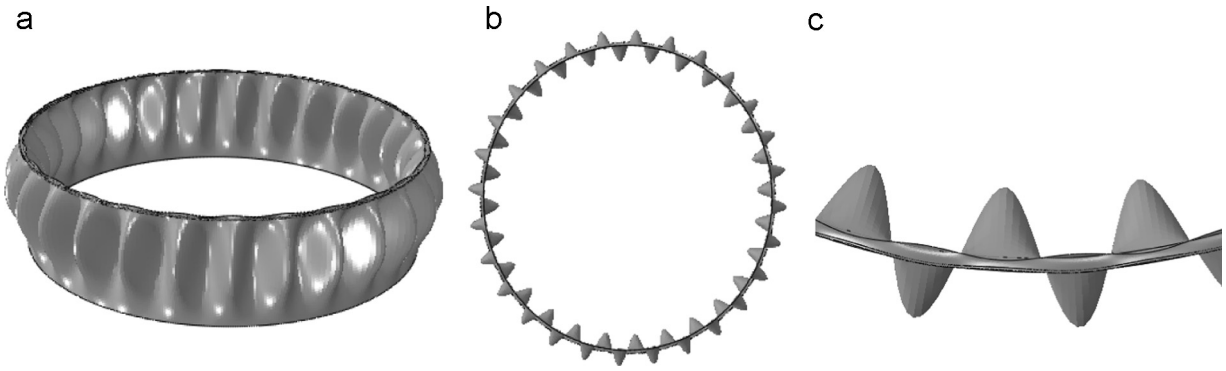

Fig. 16. First critical mode with wind girder under uniform pressure ($p^C = 3.14$ kN/m^2), for the exact girder model. (a) Side view, (b) top view, and (c) detail of deformation at the top edge.

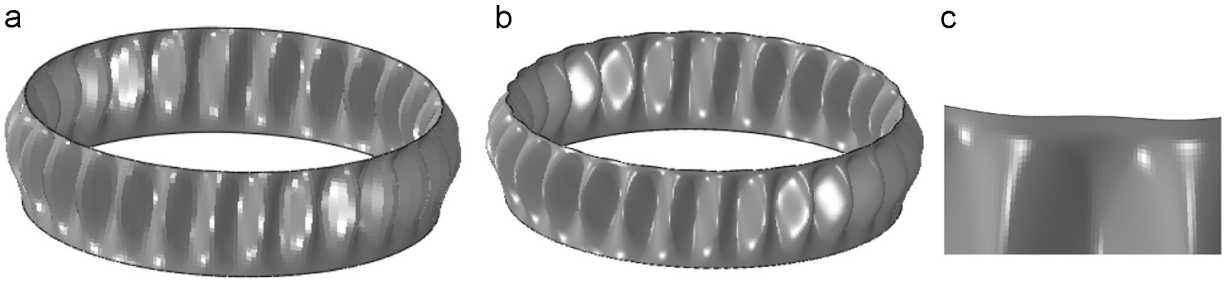

Fig. 17. First critical mode under uniform pressure, (a) simplified model with boundary condition at the top ($p^C = 3.06$ kPa), (b) equivalent thickness model ($p^C = 3.25$ kPa), and (c) detail of deformation at the top edge.

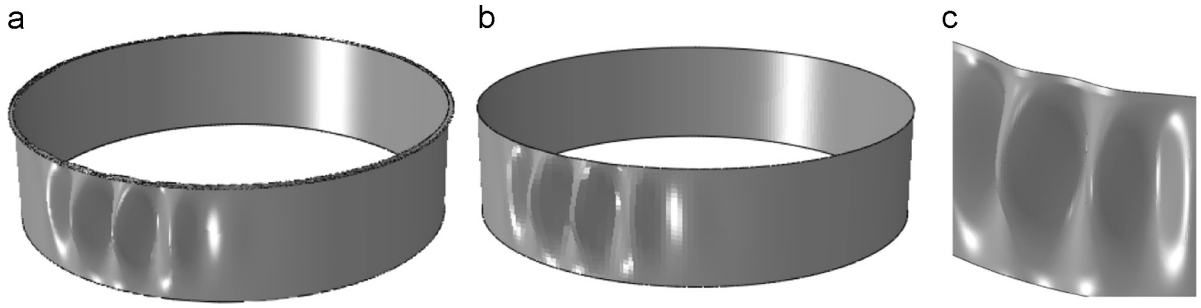

Fig. 18. First critical mode under wind, (a) tank with wind girder ($p^C = 3.38$ kPa), (b) equivalent thickness model ($p^C = 3.47$ kPa), and (c) detail of deformation at the top edge for equivalent thickness model.

assumed boundary conditions provides $p^C = 3.28$ kPa (3.1% lower than the exact value). The bifurcation modes are similar in all cases, as shown in Fig. 18b.

4. Conclusions

The consequences of introducing simplifications in the analysis of thin-walled oil storage tanks on buckling loads and modes have been discussed in this work by means of computational analysis. Two basic ways in which a shell structure is simplified in practice and research are by means of a modification in the thickness to represent some additional structural features, or by introduction of an artificial boundary condition. In the first case, changes in the density of the material need to be introduced; however, it is shown that a modified density or neglecting the roof weight does not substantially modify the results.

For a fixed roof with a supporting structure, a model in which the supports are eliminated and the roof thickness is modified to obtain the same moment of inertia lead to an equivalent thickness of 2.25 the thickness at the top of the cylinder. For thermal loads, the simplified results are 7% lower than the exact model, and the differences increase with increasing equivalent thickness. Under uniform pressure, the first cylinder mode gives results 14% lower than in the exact model. Finally, the simplified model under wind is 12% lower than in the exact model. In the three loading cases, the exact solution is recovered for large equivalent thickness values of 27 t_{bottom} for temperature load; 24 t_{bottom} for pressure; and 40 t_{bottom} for wind. Mode shapes are well described provided a cylinder mode is considered.

For an open tank with a wind girder, the equivalent thickness results in 4.75 t_{top}. Predictions under temperature are the same for exact and equivalent thickness models; for uniform pressure the equivalent thickness is 3.5% higher than the exact value; whereas the difference is 2.7% under wind.

Substituting the wind girder by a boundary condition yields poor results under thermal loads, but differences of 2.5% lower for pressure and 3.1% lower for wind are computed.

The models discussed in this work do not represent bounds: depending on the configuration, the equivalent thickness model may yield lower or higher values than exact.

Depending on the load case, for a fixed roof the differences are between 7% and 14%, and reduce to about 3% for opened tanks under pressures (either uniform or wind).

A limitation of this study is that only bifurcation loads have been evaluated, and more refined results would be obtained via geometrically nonlinear analysis with imperfections. However, interest in this work concentrates on the differences between a model that represents all details of a fixed roof or wind girder and a simplified version in which equivalent thicknesses or boundary conditions are employed. Such differences would be reflected in bifurcation as well as in nonlinear analyses.

Acknowledgments

RCJ thanks the support during this research received through grants from the National University of Comahue (SECYT-UNCo). LAG thanks the support received through grants from the National University of Cordoba (SECYT-UNC) and CONICET (PIP112-201201-00126-CO).

References

[1] Landucci G, Gubinellia G, Antonioni G, Cozzani V. The assessment of the damage probability of storage tanks in domino events triggered by fire. Accid Anal Prev 2009;41:1206–15.
[2] Liu Y. Thermal buckling of metal oil tanks subject to an adjacent fire. Ph.D. thesis. Scotland: University of Edinburgh; 2011.
[3] Zhao Y, Cao QS, Su L. Buckling design of large circular steel silos subject to wind pressure. Thin-Walled Struct 2013;73:337–49.
[4] Cao QS, Zhao Y. Buckling strength of cylindrical steel tanks under harmonic settlement. Thin-Walled Struct 2010;48(6):391–400.
[5] Gong J, Cui W, Zeng S. Buckling analysis of large scale oil tanks with a conical roof subjected to harmonic settlement. Thin-Walled Struct 2012;52(7):143–8.
[6] Jørgensen F. Buckling behavior of a liquid storage tank. Thin-Walled Struct 1983;1:309–23.
[7] API. Standard 650, welded steel tanks for oil storage. Washington, D.C.: American Petroleum Institute; 2010.
[8] British Standards, Specification for the design and manufacture of site built, vertical, cylindrical, flat-bottomed, above ground, welded, steel tanks for the storage of liquids at ambient temperature and above, British Standard 14015, London, 2004.
[9] Schmidt H, Binder B, Lange H. Postbuckling strength design of open thin-walled cylindrical tanks under wind load. Thin-Walled Struct 1998;31:203–20.
[10] Zhao Y, Lin Y. Buckling of cylindrical open-topped steel tanks under wind load. Thin-Walled Struct 2014;79:83–94.
[11] Chen L, Rotter JM. Buckling of anchored cylindrical shells of uniform thickness under wind load. Eng Struct 2012;41:199–208.
[12] Aghajari S, Abedi K, Showkati H. Buckling and post-buckling behavior of thin walled cylindrical steel shells with varying thickness subjected to uniform external pressure. Thin-Walled Struct 2006;44:904–9.
[13] Persson H, Lönnermark A. Tank fires: review of fire incidents 1951-2003. Borås, Sweden: Swedish National Testing and Research Institute; 2004.
[14] Chang JI, Lin ChC. A study of storage tank accidents. J Loss Prev Process Ind 2006;19:51–9.
[15] Godoy LA. Performance of Storage Tanks in Oil Facilities Following Hurricanes Katrina and Rita. ASCE J Perform Constr Facil 2007;21(6):441–9.
[16] Buckling of steel shells: European design recommendations. In: Rotter JM, Schmidt H, editors. 5th edition. European Convention for Constructional Steelwork, Mem Martins, Portugal; 2008.
[17] ABAQUS v6.9. Simulia. Unified FEA. Dassault Systemes. Warwick, Rhode Island. USA, 2009.
[18] Liu Y, Chen JF, Rotter JM, Torero JL Buckling of oil tanks under elevated temperature. In: Proceedings of the 5th European conference on steel and composite structures, Graz, Austria; 2008, p. 1527–32.
[19] Liu Y, Chen JF, Rotter JM, Torero JL. Buckling analysis of an oil tank exposed to heating from an adjacent tank fire. In: Proceedings of the 13th International Conference on structural faults+repair, Edinburgh, UK; 2010, 12 pp.
[20] Godoy LA, Batista-Abreu J. Buckling of fixed roof aboveground oil storage tanks under heat induced by an external fire. Thin Walled Struct 2012;52:90–101.
[21] Brush DO, Almroth BO. Buckling of bars, plates, and shells. New York, NY: MacGraw-Hill; 1975.
[22] AS/NZS. Structural Design Actions, Part 2 – Wind Actions, Australian/New Zealand Standards 1170.2:2011, Sydney: 2011.